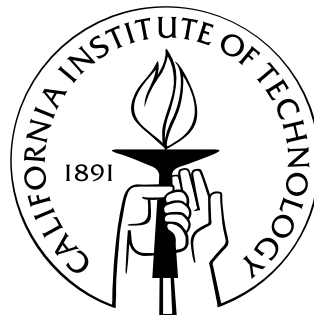


Photonic whispering-gallery resonators in new environments

Thesis by
Eric Paul Ostby

In Partial Fulfillment of the Requirements
for the Degree of
Doctor of Philosophy



California Institute of Technology
Pasadena, California
2009

(Defended May 20, 2009)

© 2009
Eric Paul Ostby
All Rights Reserved

Acknowledgements

I have immensely enjoyed my time at Caltech, it has been the most challenging and rewarding experience in my life. I owe a debt of gratitude to the many people who contributed to my maturity as a researcher and analytical thinker at Caltech. I would like to first thank my advisor Professor Kerry Vahala. He expertly guided me to success in the many projects I worked on, and I have benefited from his intelligence, creativity, and rigorous approach to science. In spite of his busy schedule, Kerry always made time for individual meetings and easily moved between projects offering insightful advice. Also, Rosalie deserves praise for her fast resolution of any administrative matters and kindness.

No researcher works in a bubble, and so it was in my graduate career. I thank my fellow group members who offered open ears, suggestions, or even their time to help me – Mani Hossein-Zadeh, Lan Yang, Tao Lu, Andrea Armani, Bumki Min, Hansuek Lee, Ivan Grudin, and Tong Chen. I thank Mani for his advice and mentorship, I based my vacuum chamber design on the first vacuum chamber that he built. Mani and I spent many hours together at Caltech, and I am thankful for the strong friendship we formed. Just when Mani was leaving to become professor, Hansuek Lee joined the group and we formed a close friendship as well. Hansuek taught me advanced fabrication techniques and generously collaborated on the spiral and vacuum reflow projects. I am especially thankful for his help during the last months before graduation, and have enjoyed spending time with him and his growing family. I would also like to thank Joyce Poon for insightful discussions on plasmonics and help with metal evaporation. Raviv Perahia lightened up challenging research with jokes, and also selflessly giving his time to take SEM images.

I cannot imagine my years at Caltech without my two closest friends, Jim Adleman and Johnny Green. Jim and I worked together in Professor Dimitri Psaltis' group for two years, and formed a lifelong bond. I thank Jim for his unwavering support of me – in my research, at Raytheon, and at my wedding in Rio de Janeiro. We shared many laughs, cold pints, and lopsided defeats in GSC basketball games. Johnny and I quickly became great friends, celebrated our Norwegian heritage, and were roommates for one year. Johnny has been a constant companion – encouraging me through the challenges of doctoral research, supporting me as I courted my wife from long distance, and spotting my bench presses. Jim and Johnny are wonderful friends, and they have painted a rich fabric of memories that I will never forget. I also thank all of my other friends, each of you has brightened my day and made my Caltech experience amazing. The students, faculty, and staff at Caltech are brilliant, providing for a diverse and stimulating intellectual environment.

My dream of achieving a doctoral degree in engineering was only possible with the lifelong love and formation I received from my parents, John and Sandy. I thank them for their tireless support, trips to see me, and understanding of the challenges I faced. My parents are my heroes – they have given me not only the academic rigor and work ethic necessary to succeed, but most importantly

they taught me to be a kind person, to love all good things. Also, I am thankful for the support and love I have received from my brother and sisters – Anna, Tim, Janelle, and Katrina.

Finally, I am most grateful to my wonderful wife Maria Fernanda Oppermann Bento. She has supported me throughout my graduate career, encouraged me on the hard days, and celebrated with me on the good ones. She always showed great interest in my research, and even helped me on several experiments. I am blessed by her love everyday, and thank her for all the sacrifices she has made for us. I respect my wife a great deal, and admire her sensitive heart and kindness towards others. I dedicate this thesis to Fernanda, my true love.

Eric Ostby
May 2009
Pasadena, CA

Abstract

Optical whispering-gallery devices, like the microtoroid or microdisk, confine light at resonant frequencies and in ultra-small volumes for long periods of time. Such ultra-low loss resonators have been applied in diverse areas of scientific research, including low-threshold lasers on-chip, biological sensing, and quantum computing. In this thesis, novel ultra-low loss microstructures are studied for their unique characteristics and utility. The author investigates the interaction between micro-cavities and various environments in order to quantify the results and lay the foundation for future applications.

The first optical cavity studied is the microtoroid, which possesses ultra-high quality factor (Q) on account of its nearly atomic smooth surface, produced by surface-tension induced laser reflow. Ytterbium-doped silica microtoroids are fabricated by a sol-gel technique. The ytterbium microtoroid laser achieves record-low laser threshold ($2 \mu\text{W}$) in air, and produces the first laser output for a solid-state laser in water. This laser in water can be developed as an ultra-sensitive biological sensor, with potentially record sensitivity enabled by gain-narrowed linewidth. Also, a novel CO_2 laser reflow and microtoroid testing vacuum system is demonstrated. Fabrication and testing of microtoroids is performed in a vacuum chamber to study the effect of atmospheric water and upper limit of Q in microtoroids.

The selective reflow of microtoroids presents difficulties for integration of on-chip optical waveguides. As an alternative, dimension-preserving low-loss optical structures are researched for their unique applications. A gold-coated silica microdisk is fabricated, and demonstrates record and nearly-ideal quality factor (1,376) as a surface-plasmon polariton resonator. The hybrid optical-plasmonic mode structure is studied in simulation and experiment. The plasmonic resonator has ultra-low mode volume and high field confinement, making it suitable for short-range optical communication or sensing. Finally, a novel whispering-gallery optical delay line in a spiral geometry is designed and experimentally demonstrated. The center transition region of the spiral is optimized for low transmission loss by beam propagation simulation. A 1.4 m long spiral waveguide within a 1 cm^2 area is presented. The spiral waveguide structure is being developed as a real-time optical delay line with fiber-like loss, important for optical communication and signal processing.

Contents

List of Figures	xi
List of Publications	xv
1 Introduction	1
1.1 Microcavities	1
1.2 Thesis outline	2
2 Ultra-high Q microtoroid	5
2.1 Microtoroid resonator overview	5
2.1.1 Whispering-gallery mode structure	6
2.2 Microtoroid fabrication	10
2.2.1 Photolithography and wet etching	10
2.2.2 CO ₂ laser reflow	12
2.3 Experimental testing of microtoroids	13
2.3.1 Low-loss optical fiber coupling to microcavities	13
2.3.2 Quality factor	15
2.3.3 Thermal broadening	18
2.3.4 Inverse thermal broadening	20
2.4 Summary	22
3 Ultralow-threshold ytterbium-doped glass laser fabricated by the solgel process	23
3.1 Introduction	23
3.2 Solgel fabrication of silica thin-films	24
3.2.1 Sol synthesis by hydrolysis	24
3.2.2 Gel synthesis by condensation	25
3.2.3 Glass densification by heat treatment	25
3.3 Ytterbium activated silica for laser gain	26
3.3.1 Electronic structure of ytterbium	26

3.3.2	Ytterbium laser characteristics	26
3.4	Yb:SiO ₂ laser modeling	28
3.4.1	Laser model parameters	28
3.4.2	Laser pump threshold	29
3.4.3	Laser model results	29
3.5	Yb:SiO ₂ laser fabrication	34
3.5.1	Silica thin film preparation by the solgel method	34
3.5.2	Microtoroid fabrication	34
3.6	Laser testing	35
3.6.1	Experimental setup	35
3.6.2	Ytterbium concentration	35
3.6.3	Laser results	37
3.6.4	Saturable absorption induced laser pulsing	39
3.7	Summary	39
4	Yb-doped glass microcavity laser operation in water	41
4.1	Introduction	41
4.2	Fabrication of microtoroid for laser in water	41
4.3	Laser testing in water	42
4.4	Summary	47
5	High-Q surface plasmon-polariton microcavity	49
5.1	Introduction	49
5.1.1	Plasmonics	49
5.1.2	Surface plasmon polaritons	50
5.1.3	Plasmon resonator concept	50
5.2	Microtoroid plasmonic resonator	50
5.2.1	Fabrication of metal coated microtoroid resonator	51
5.2.2	Microtoroid resonator results	51
5.3	Microdisk based plasmonic resonator	54
5.3.1	Plasmonic disk resonator fabrication	54
5.4	Finite-element model of SPP resonator	56
5.4.1	Fiber and SPP resonator phase matching	58
5.4.2	SPP resonator quality factor	59
5.5	Plasmonic resonator results	60
5.5.1	Testing setup	60
5.5.2	Measured quality factors	60

5.5.3	SPP modes dependence on coupling	62
5.6	Application of SPP resonator	64
5.7	Summary	64
6	Microtoroid reflow and measurement in vacuum	67
6.1	Introduction	67
6.2	Sources of loss in microtoroids	68
6.2.1	Intrinsic loss	68
6.2.2	Whispering gallery loss	68
6.2.3	External sources of loss	69
6.3	Microtoroid loss caused by water	70
6.4	Vacuum reflow system	71
6.4.1	Vacuum chamber	72
6.4.2	CO ₂ laser annealing	73
6.4.3	Microtoroid testing	74
6.5	Vacuum reflow system assembly	74
6.6	Microtoroid reflow and testing in vacuum	77
6.7	Summary	80
7	Additional research into novel whispering-gallery devices	81
7.1	Introduction	81
7.2	Spiral delay line	81
7.2.1	Spiral waveguide design	84
7.2.2	Spiral waveguide fabrication	87
7.2.3	Spiral waveguide measurement	89
7.3	Short-pulse microcavity laser	90
7.3.1	Laser concept	90
7.3.2	Pulsed laser modeling	91
7.4	Microtoroids for atom cavity experiments	93
7.4.1	Cavity quantum electrodynamics	94
7.4.2	Experimental details	95
7.4.3	Demonstration of anti-bunching and sub-Poissonian statistics	95
7.4.4	High efficiency single photon routing	95
7.4.5	Fabrication of small mode volume UHQ microtoroids for cQED research	96
7.4.6	Vacuum reflow of microtoroids for cQED	96
7.5	Summary	96

List of Figures

2.1	SEM image of microtoroid resonator	6
2.2	Plot of the electric field intensity profile $ E_\phi ^2$ of a 120 μm diameter toroid (generated by FEM model)	7
2.3	Diagram of a toroid with field components in cylindrical coordinates for the TM-type whispering-gallery modes	8
2.4	Diagram of the fabrication steps of silica microtoroids	10
2.5	Plot of the experimental etch rate of silicon ($\Delta D/\Delta T$) as a function of pillar diameter for one microdisk	11
2.6	Image of a broadband bent fiber taper, the taper diameter is 5 μm in the narrowest section, and the loop diameter is 50 μm	14
2.7	Top view image of microtoroid and fiber taper	15
2.8	Measurement of cavity Q by resonance linewidth, showing a UHQ microtoroid doublet mode	17
2.9	Measurement of microtoroid Q by cavity ringdown	17
2.10	Plot of taper transmission showing normal thermal broadening for a microtoroid	19
2.11	Plot of taper transmission during laser scan showing inverse thermal broadening for a PMMA coated microtoroid	21
3.1	Energy level diagram for $\text{Yb}^{3+}:\text{SiO}_2$	27
3.2	Absorption and emission cross-sections of $\text{Yb}^{3+}:\text{SiO}_2$	27
3.3	Plot of $\text{Yb}:\text{SiO}_2$ laser threshold as a function of ytterbium concentration (N_T) for a $D = 43 \mu\text{m}$ microtoroid (model predictions)	31
3.4	Plot of $\text{Yb}:\text{SiO}_2$ laser threshold as a function of toroid major diameter (mode predictions)	32
3.5	Comparison of $\text{Yb}:\text{SiO}_2$ laser Q at the pump resonance as a function of the Yb concentration (model and experimental results)	33
3.6	Top-view photograph of testing setup showing evanescent coupling of fiber taper to $\text{Yb}^{3+}:\text{SiO}_2$ microtoroid laser	35

3.7	Measured laser threshold (absorbed power) as a function of Yb^{3+} concentration for Yb-doped silica microcavity.	36
3.8	Measured laser output power as a function of absorbed pump power for two $\text{Yb}^{3+}:\text{SiO}_2$ microtoroid lasers	37
3.9	Measured laser output spectra of single-frequency $\text{Yb}^{3+}:\text{SiO}_2$ microtoroid laser . . .	38
3.10	Plot of toroid laser pulsing caused by saturable absorption of unpumped Yb^{3+} ions .	38
4.1	Image of $\text{Yb}:\text{SiO}_2$ laser coupled to a fiber taper (side view)	43
4.2	Diagram of the setup for testing in water (side view)	44
4.3	Plot of microtoroid pump resonance in water ($Q = 1.3 \times 10^5$)	45
4.4	Comparison of measured laser output power as a function of absorbed pump power for 120 μm diameter $\text{Yb}^{3+}:\text{SiO}_2$ microtoroid in air and water	46
4.5	Plot of laser output in water at low pump powers showing the laser threshold	46
5.1	Microscope image of a silica microtoroid coated with 200 nm gold coating (top view)	51
5.2	Plot of fiber taper transmission versus wavelength of coupling to a gold coated microtoroid showing the mode spectrum	52
5.3	Plot of the dielectric cavity mode of a gold-coated microtoroid generated by FEM simulation	53
5.4	Tapered fiber waveguide and SPP whispering-gallery microdisk resonator	55
5.5	Cavity mode dispersion	57
5.6	Effective cavity mode indices	58
5.7	The theoretical Q factor for SPP_{1m} , plotted as a function of microdisk's azimuthal mode number, m	59
5.8	Q -factor measurements for silver-coated and chromium-coated microdisk resonators .	61
5.9	Transmission spectrum versus waveguide coupling gap	63
6.1	Schematic diagram of vacuum reflow concept	72
6.2	Image of CO_2 laser optics and vacuum chamber	75
6.3	Image of laser and imaging beam combiner	75
6.4	Image of microtoroid reflow and coupling setup inside a vacuum chamber	76
6.5	Resonance linewidth measurement of Q in vacuum for a microtoroid doublet mode .	78
6.6	Ringdown measurement of microtoroid Q in vacuum	79
7.1	Stereo-microscope image of 1.4 m long silica waveguide in spiral geometry defined within $< 0.4 \text{ cm}^2$ area	82
7.2	SEM image of a 20 μm diameter silica microdisk with bevel	83

7.3	Comparison of the WGM field pattern for a microtoroid (left) and a wedged microdisk (right)	83
7.4	Single arm Archimedean spiral, two arms are joined to form the complete spiral . . .	84
7.5	Field distributions of positive and negative spiral spatial modes	85
7.6	Plot of the center s-bend design for high transmission in a spiral waveguide	87
7.7	SEM image of the center portion of one completed spiral	88
7.8	SEM image of a cleaved spiral showing the waveguide cross-section with sidewall bevel and silicon support	88
7.9	Top view of single turn two arm spiral with dual fiber taper coupling for transmission measurement	90
7.10	Plot of the Cr,Yb:SIO ₂ microtoroid pulse duration as a function of Cr ⁴⁺ concentration.	92
7.11	Plot of the pulsed laser threshold as a function of Cr ⁴⁺ concentration.	93
7.12	Schematic of microtoroidal resonator and fiber coupler	94

List of Publications

Portions of this thesis have been drawn from the following publications:

Yb-doped glass microcavity laser operation in water E. Ostby and K. Vahala, Optics Letters, **34**, 1153–1155 (2009).

High-Q surface-plasmon-polariton whispering-gallery microcavity B. Min, E. Ostby, V. Sorger, E. Ulin-Avila, L. Yang, X. Zhang, and K. Vahala, Nature, **457**, 455–458 (2009).

Ultralow-threshold $\text{Yb}^{3+}:\text{SiO}_2$ glass laser fabricated by the sol-gel process E. Ostby, L. Yang, and K. Vahala, Optics Letters, **32**, 2650–2652 (2007).

A Photon Turnstile Dynamically Regulated by One Atom B. Dayan, A. Parkins, T. Aoki, E. Ostby, K. Vahala, and H. Kimble, Science, **319**, 1062–1065 (2008).

Efficient routing of single photons by one atom and a microtoroidal cavity T. Aoki, A. Parkins D. Alton, C. Regal, B. Dayan, E. Ostby, K. Vahala, and H. Kimble, Physical Review Letters, **102**, 083601 (2009).

Wavelength-independent coupler from fiber to an on-chip cavity, demonstrated over an 850nm span T. Carmon, S. Wang, E. Ostby, and K. Vahala, Optics Express, **15**, 7677–7681 (2007).

